Special Focus, Ocular Oncology and Pathology, Original Article

Pathologic evidence of retinoblastoma seeds supported by field emission scanning electron microscopy and Raman spectroscopy

Dipankar Das, Kasturi Bhattacharjee[1], Manab J Barman[2], Harsha Bhattacharjee[3], Surjendu Maity[4], Dipankar Bandyopadhyay[4], Siddharth Thakur[4], Saurabh Deshmukh[2], Mohit Garg[3], Apurba Deka[5]

Purpose: The aim of this study was to examine the pathology of retinoblastoma (RB) seeds with supportive evidence by field emission scanning electron microscopy and Raman spectroscopy. **Methods:** This study was a laboratory-based observational study. Enucleated eyeballs received in the ocular pathology department of a tertiary eye care center in northeast India were included in the cohort after obtaining written informed consent during the surgery. The study was carried out for 6 years (2015–2020). Most of the eyeballs were Group-E RBs. Standard eyeballs sectioning were done by bread loaf techniques. Gross documentations included RB seeds seen in the smallest calotte done with utmost care. Seeds were documented also in permanent sections. Scanning electron microscopy and Raman spectroscopy were carried out in an index case. **Results:** Out of the total 59 cases, 35 RB cases had different seedings. The mean age at enucleation was 2.9 years. RB seeds were seen in vitreous (n = 19), subretinal plus vitreous (n = 7), anterior chamber (n = 1), over crystalline lens (n = 3), retinal surface (n = 1), retinal pigment epithelium (RPE; n = 2), subretinal (n = 1), calcified seeds (n = 2). Other characteristics were dusts (n = 7), clouds (n = 11), spheres (n = 4), and unspecified type (n = 13). Histopathological high-risk factors showed significant choroidal (n = 22) and optic nerve (n = 15) involvement. Few cases had extraocular spread. Undifferentiated tumor (n = 24) was seen with higher evidence of necrosis (n = 23). Raman spectra differentiated the seeds from the normal tissue on the basis of lipid and protein content. **Conclusion:** This study highlights the different types of RB seeds with high-risk factors. The morphology of those seeds showed the difference between vitreous and subretinal seeds under advanced microscopic observations.

Access this article online

Website: www.ijo.in

DOI: 10.4103/ijo.IJO_436_21

Quick Response Code:

Key words: Electron microscopy, fluorescein, pathology, retinoblastoma, Raman spectroscopy, seeds

Retinoblastoma (RB) is the most common primary intraocular malignancy in children accounting for 3% of all childhood cancers.[1-13] RB seedings had been studied clinically and pathologically in the past.[4,10,12,13] They have a lot of significance in the spreading of RB to the adjoining areas and extraocularly.[4,10,12,13] Vitreous seeds had been classified earlier by Munier[12] in 2013 as dusts, clouds, spheres, and mixed types.[12] Seeds were further grouped as prehyaloids, subhyaloids, epiretinal, intraretinal, and subretinal seeds.[12,13] Anterior chamber seeds could be depository or infiltrative.[12,13] We studied the pathological significance of RB seeds with histopathological risk factors. Field emission scanning electron microscopy (FESEM) for seeds, calcifications,[14-16] and Raman spectroscopy [17-20] were studied in an index case in the cohort with interesting observations.[17-20]

Methods

The aim of this study was to examine the pathology of RB seeds with supportive evidence by FESEM and Raman spectroscopy.

The pathological reports that included grossing and microscopic findings were collected from the ocular pathology laboratory of a tertiary eye care center of northeast India between 2015 and 2020. In total, 59 cases of RB were included in the study. Out of which 35 cases (59.33%) had different RB seeds. Approval of Institutional Ethics Committee for the study was obtained, dated 12.01.2019.

The design of the study was retrospective and laboratory based where written informed consents were obtained from all the patients' guardians before enucleating the eyes.

The enucleated eyeballs, mostly Group-E RBs received in the laboratory in 10% neutral buffer formalin and was fixed for 48 hours. They were measured in different dimensions,

Departments of Ocular Pathology, Uveitis and Neuro-Ophthalmology, [1]Oculoplasty, Cataract and Refractive Surgery, [2]Vitreo-Retina, [3]Ophthalmology and [5]Ocular Pathology, Sri Sankaradeva Nethralaya, Guwahati, [4]Centre for Nanotechnology and Department of Chemical Engineering, Indian Institute of Technology, Guwahati, Assam, India

Correspondence to: Dr. Dipankar Das, Senior Consultant and HOD: Uveitis-Ocular Pathology Services, Department of Ocular Pathology, Uveitis and Neuro-Ophthalmology, Sri Sankaradeva Nethralaya, 96 Basistha Road, Beltola, Guwahati, Assam, India. E-mail: dr_dasdipankar@yahoo.com

Received: 21-Feb-2021 Revision: 07-Jun-2021
Accepted: 06-Jul-2021 Published: 26-Nov-2021

Cite this article as: Das D, Bhattacharjee K, Barman MJ, Bhattacharjee H, Maity S, Bandyopadhyay D, *et al.* Pathologic evidence of retinoblastoma seeds supported by field emission scanning electron microscopy and Raman spectroscopy. Indian J Ophthalmol 2021;69:3612-7.

including eyeballs, cornea, pupil, and optic nerve. The cut ends of the optic nerves were submitted separately. Transillumination were done in RB eyeball specimens to know the position of the intraocular mass so that the dissection can be carried out in a particular plane to have optimum tumor samples.

The cut sections of the eyeballs were examined meticulously with the measurement of tumor dimensions and noting down the different gross pathologies. The other halves of the eyeballs were cut by bread loaf technique[9] and photographed under grossing microscopy (Leica S6D, Germany). The peripheral calotte, which was smaller in size, were stained with a drop of freshly obtained sodium fluorescein ($C_{20}H_{12}O_5Na$) solution (10%) containing 500 mg of fluorescein in 5 mL.[10] They were seen under the objectives of a compound microscope (Axioskop 40, AxioCam MRc ZEISS, Germany). Different RB seeds in various locations were documented. After the digital documentations, the calotte tissues were dipped gently in the same formalin and water to wash the excess fluorescein, and the specimens were transferred to the processing cassettes immediately and fixed further in 10% neutral buffered formalin. Special care was taken to avoid distortions of the tissues, and the entire procedure was rapidly done without any tissue drying.[10] In all 35 cases, age, gender, eyes involved, types of tumor, and risk factors including anterior chamber, uveal tissue, RPE, optic nerve, episcleral, scleral, and orbital involvements were noted. Differentiations of the tumor, necrosis, calcifications, and anaplasia were also correlated with the RB seeds. RB seeds were furthered grouped into anterior chamber, lens, vitreous, retinal, RPE, subretinal, and combinations of vitreous and subretinal seeds. Furthermore, RB seeds were classified on the basis of dusts, clouds, spheres, and unspecified ones.

FESEM of RB seeds and tumoral calcifications were done at the Indian Institute of Technology, Guwahati (IITG). Raman spectroscopy in one of the cases was also done at that institute. Paraffin-embedded third calotte of one of the specimens was selected after its complete histopathological reporting. Wax was melted from paraffin-embedded tissue and was cleaned thoroughly in 2% glutaraldehyde and transferred to the IITG nanotechnology laboratory. To prepare samples for FESEM analysis at IITG, the RB seeds containing tissue were placed over the blank glass slide, which was further positioned on the sample holder by using carbon tape. After that the setup was dried overnight at the normal temperature inside a vacuum desiccator followed by the coating with platinum through plasma sputter before use. The FESEM (JEOL, JSM-7610F, Tokyo, Japan) was used to study the surface morphology of the RB seeds. Different functional groups present on the RB seeds were confirmed by Raman spectroscopy (Horiba Jobin Vyon, Model LabRam HR, Tokyo, Japan). For this purpose, the RB seeds were placed over the blank glass slide before use and then spectroscopy was carried out and analyzed.

Results

In the 6 years study period (2015–2020), the total RB cases seen in enucleated eyeballs were 59, and out of that 35 cases had different RB seedings at different locations. In all 35 cases, the mean age of RB children with different seeds was 2.9 years. There were 17 males and 18 females. Right eye (OD) outnumbered the left eye (OS) in the ratio of 25:10. With respect to the types of tumor, endophytic growth was seen in 28 cases (80%), exophytic in one case (2.86%), and a combination of endophytic and exophytic growth was seen in one case (2.86%). Unspecified growth types were seen in five cases (14.29%). Histopathological high-risk factors showed anterior chamber involvement in two cases (5.72%), iris neovascularization and tumor involvement in two cases (5.72%), and ciliary body involvement in one case (2.86%). The choroid was involved in lateral calottes in 22 cases (62.86%), where 17 were focal cases (48.58%) and five cases (14.29%) had massive choroidal involvement. Optic nerves were involved in 15 cases (42.86%) – prelaminar four cases (11.43%); postlaminar two cases (5.72%), and cut end of the optic nerve nine cases (25.72%). Episcleral involvement was seen in one case (2.86%) with scleral and extrascleral involvement in two cases each (5.72%). Orbital involvement was seen in one case (2.86%). In one isolated case, tumor involvement was seen in RPE (2.86%). In the differentiation of RBs, 24 cases (68.57%) were undifferentiated and two cases (5.72%) were differentiated RBs. Necrosis was seen in 23 cases (65.72%) with intratumoral calcifications in 19 cases (54.29%) and tumor anaplasia in 17 cases (48.57%). Exudative retinal detachments were seen in 17 cases (48.57%) out of the 35 RB cases [Table 1].

Table 1: Profile of RB and seeds (2015-2020)

Features	Numbers
Total RB cases	59
RB seeds	35
Age (mean)	2.9 years
Male	17
Female	18
Right eye (OD)	25
Left eye (OS)	10
Endophytic growth	28
Exophytic growth	1
Combine growth	1
Unspecified growth	5
Anterior chamber involvement	2
Iris involvement	2
Ciliary body involvement	1
Choroidal involvement (Focal - 17; Massive - 5)	22
Optic nerve involvement (Prelaminar - 4; postlaminar - 2, Cut end ON - 9)	15
RPE Involvement	1
Episcleral involvement	1
Scleral involvement	2
Extrascleral Involvement	2
Orbital involvement	1
Undifferentiated RB	24
Differentiated RB	2
Necrosis	23
Calcification	19
Anaplasia	17
Exudative retinal detachment	17

RB=retinoblastoma, RPE=retinal pigment epithelium, ON=optic nerve

RB seeds seen in anterior chamber (n = 1, 2.86%), over crystalline lens (n = 3, 8.58%), vitreous (n = 19, 54.29%) [Fig. 1], retinal (n = 1, 2.86%), RPE (n = 1, 2.86%), subretinal (n = 1, 2.86%) [Fig. 2a and b], vitreous and subretinal together (n = 7, 20%), and calcified seeds (n = 2 cases, 5.72%). Both the calcified seeds were seen in regressed RB in phthisical eyes. Furthermore, RB seeds were classified into dusts (n = 7, 20%), clouds (n = 11, 31.43%), spheres (n = 4, 11.43%) and unspecified type (n = 13, 37.15%) [Table 2]. Fluorescein stain picked up RB seeds in gross pathological documentations in all 35 cases (100%), and hematoxylin and eosin (H and E) stain could show RB seeds in 19 cases (54.29%). In H and E-stained slides, vitreous seeds were seen in two RB cases (5.72%) accompanied by the RB rosettes described by Das *et al*.[8]

RB seeds [Fig. 3] and intratumoral calcification [Fig. 4a and b] were documented in FESEM, and the region of the Raman spectra analysis was documented [Fig. 5a and b]. Raman spectra of the RB seed[16,17] showed peaks around 784, 1,095, and 1,587 cm^{-1} confirmed the oxygen–phosphorus–oxygen (O-P-O) stretching of deoxyribonucleic acid (DNA) backbone, ring breathing mode of tyrosine, and ring breathing mode of guanine (G) and adenine (A), respectively. The peak around 1,004 cm^{-1} signified the symmetric ring breathing mode of phenylalanine. Furthermore, peaks at around 1,250, 1,340, and 1,450 cm^{-1} represented β-sheet of amide III, DNA nucleic acids adenine (A) with guanine (G) and carbon–hydrogen (C-H) deformation in proteins, and C-H deformation in all cellular components.

Discussion

RB is the most common primary intraocular malignancy in childhood, occurring in 1 in 14,000 to 20,000 live births.[1-13]

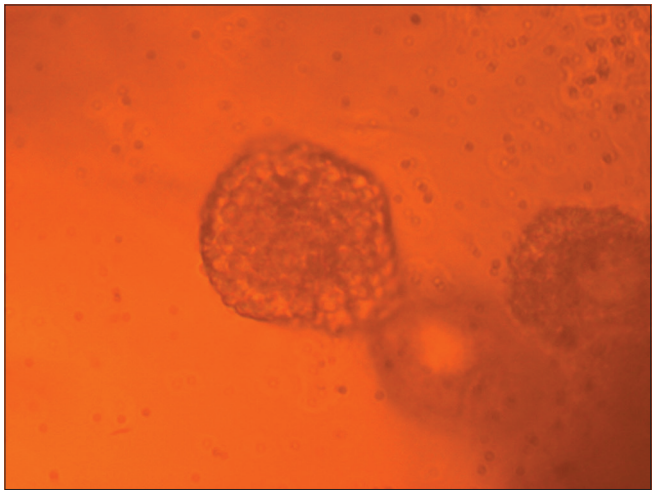

Figure 1: Fluorescein-stained gross photograph of vitreous RB seed having characteristic surface honeycomb appearance (×20)

Table 2: Showing different types RB seedings

Site (s) and types of RB seeds	Number of cases
Anterior chamber	1
Over crystalline lens	3
Vitreous	19
Retinal	1
RPE	1
Subretinal	1
Vitreous + subretinal	7
Calcified	2
Other characteristics	
Dusts	7
Clouds	11
Spheres	4
Unspecified	13

RPE=retinal pigment epithelium

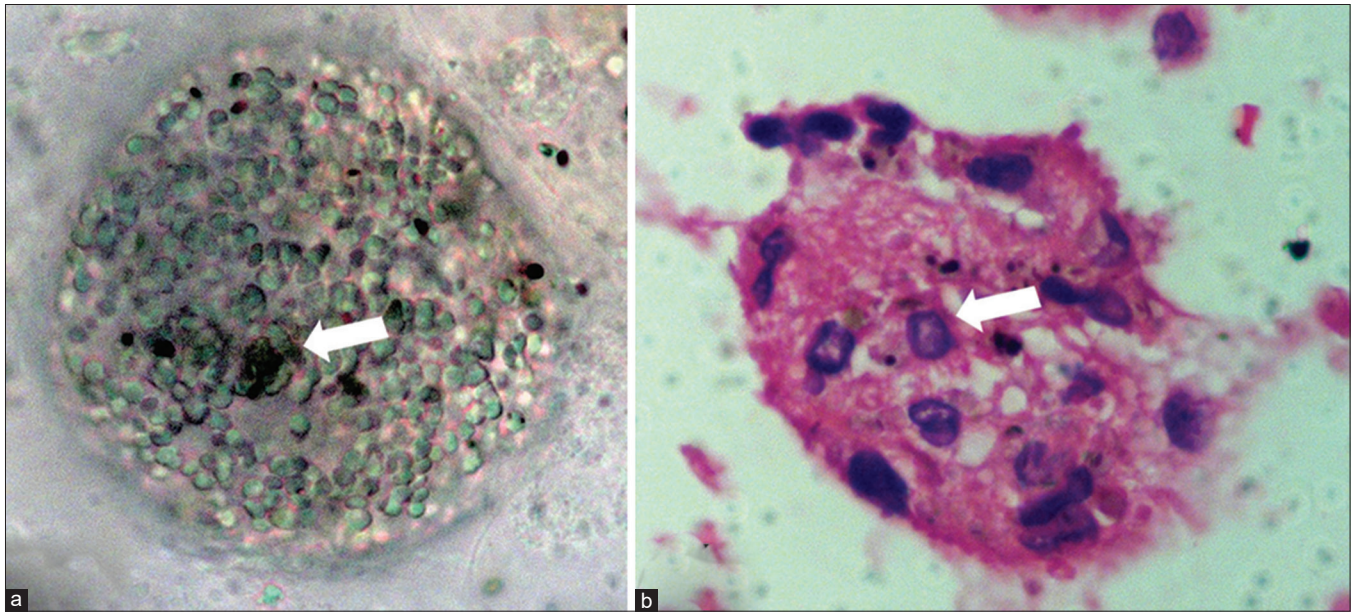

Figure 2: (a) Diffracted, white, balanced gross photograph of subretinal RB seed with surface pigmentation (arrow) (×40). (b) Similar surface change in H and E-stained slide (arrow) (×40)

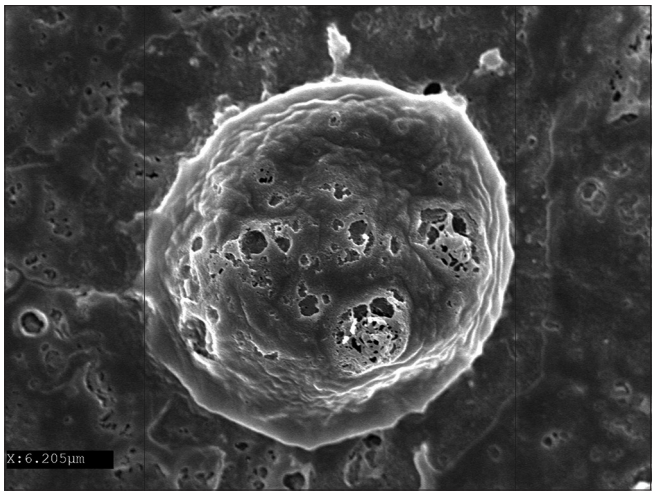

Figure 3: Single subretinal RB seed with the surface change in FESEM (×11,000)

It is a cancer of the retina that is seen as an extension of the brain to the eye.[2-11,13] RB seeds had been studied clinically and pathologically previously.[4,10,12,13] We studied the RB seeds pathologically by using fluorescein stain[10] and histopathologically, and in one case we correlated our findings with FESEM and Raman spectroscopy.

Our pathological study at a tertiary institute revealed 35 cases of RB with different seeds. The most common seeds were located in the vitreous cavity. Isolated seeds were seen in the anterior chamber, which was depository type, retinal, and subretinal tissue. Combined vitreous and subretinal seeds were seen in seven cases. Few seeds were seen on the surface of the crystalline lens along with seeds deposition on RPE. The sodium fluorescein stain technique of gross pathology developed by the author was able to document seeds in all the cases.[10] However, with H and E staining, 19 cases (54.29%) had shown seeds in the permanent section. It was thought that by tissue processing, fragile seeds were probably lost compared

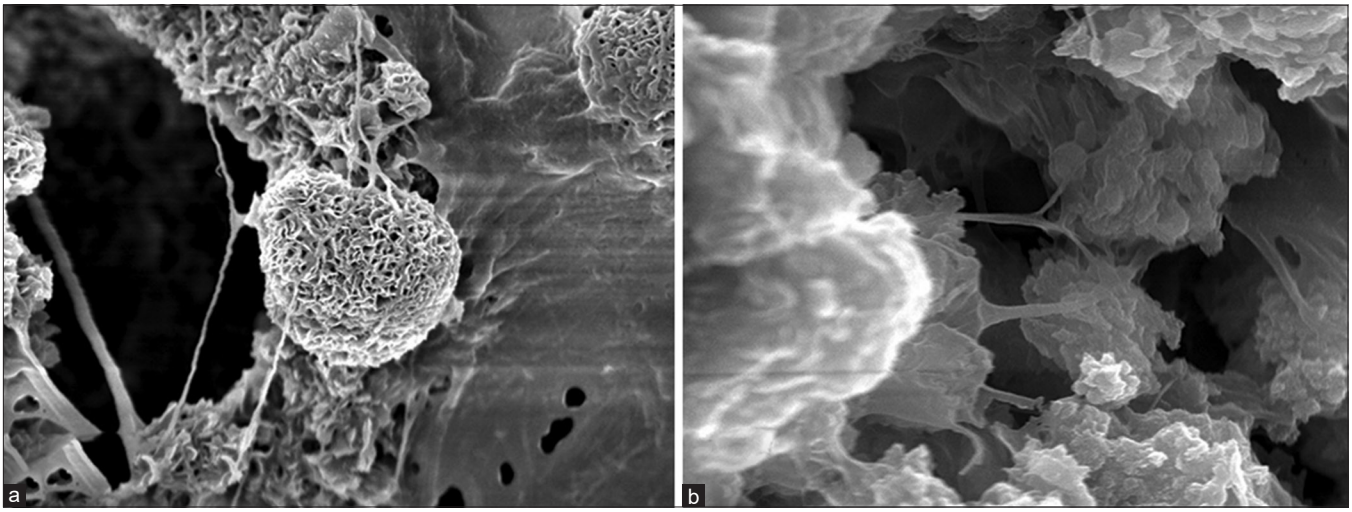

Figure 4: (a) Interlacing calcium hydroxyapatite fibers orientation in FESEM (×20,000). (b) Another zone of networking fibers of RB calcification (×20,000)

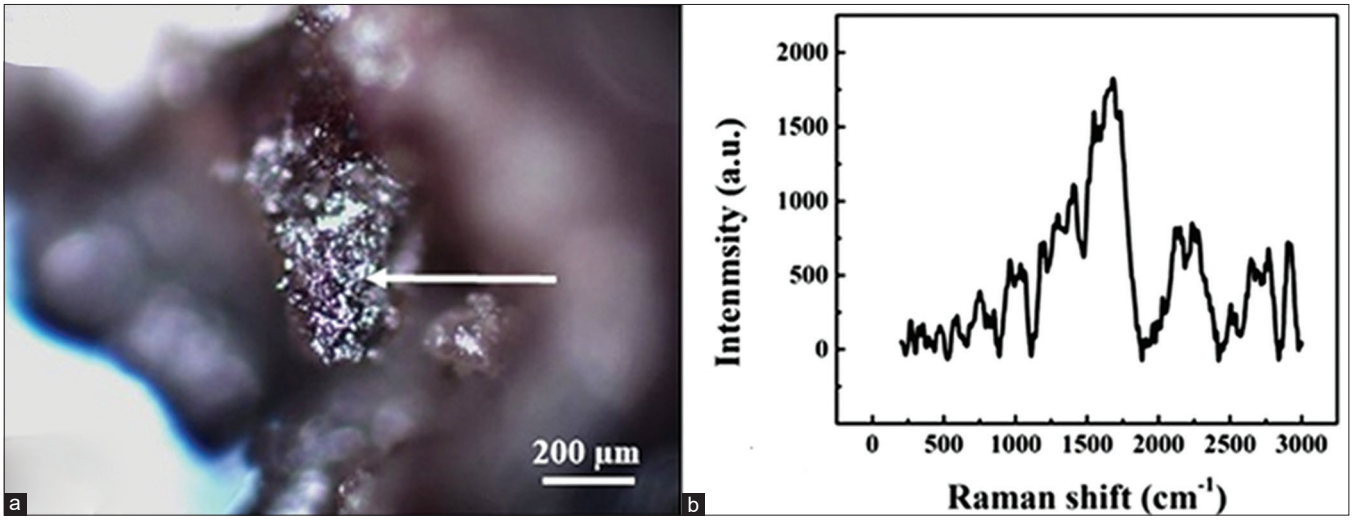

Figure 5: (a) Microscopic image of the RB seed, and the arrow indicating the region of the Raman spectra analysis. (b) Raman spectra of the RB seed. The peaks seen around 784, 1,095, and 1,587 cm^{-1} were confirmed the O-P-O stretching of DNA backbone, ring breathing mode of tyrosine, and ring breathing mode of guanine (g) and adenine (a), respectively. The peak around 1,004 cm^{-1} signified the symmetric ring breathing mode of phenylalanine. Peaks at around 1,250, 1,340, and 1,450 cm^{-1} represented β-sheet of amide III, DNA nucleic acids adenine (a) with guanine (g), C-H deformation in proteins, and C-H deformation in all cellular components. Note: Peak of the seed differed from the peak of adjoining areas

with the fresh tissue documentation. We were able to see dust seeds in seven cases, clouds in 11 cases, spheres in four cases, and unspecified seeds type in 13 cases.

The surface of vitreous RB seeds differed from subretinal ones in our study. RB seeds were correlated with other histopathological findings. Endophytic growth was the maximum in our study. High-risk histopathological factors showed significant choroidal involvements in lateral calottes of eyeball along with optic nerve involvement. The active seeds in the vitreous, subretinal, and other extraocular spaces were associated with the advancement of the cancerous growth. Undifferentiated tumors were more than the differentiated ones in our study. Tumor necrosis and anaplasia were noted in a significant number of cases. We had seen anaplasia in 17 cases. Most of the anaplasias were graded as moderate to severe (15/17 cases). Mendoza *et al*.[21] described increasing grade of anaplasia was associated with reduce overall survival and increased threat of metastasis. Histopathologic features that were associated with anaplasia included anterior segment, choroidal and optic nerve invasion. Multivariate study considering high-risk histopathology and anaplasia grading predictors of metastasis and death showed that high-risk histopathology was statistically significant as an independent predictor irrespective of anaplasia. In the absence of high risk features, however, severe anaplasia identified as an additional risk of metastasis. Therefore, the study showed that adjuvant therapy could have been required in those situations.[21] The mean age of our patients at enucleation was 2.9 years, which was also higher compared with the median age of unilateral and bilateral RBs.[1-13] Interestingly, we had seen two cases of RB with vitreous seeds associated with the new rosettes described by the author in 2014.[8,10,13]

The present study included FESEM observations of RB seeds, intratumoral calcification, and Raman spectroscopy study in a single case. This was in an enucleated eyeball in an 18-month-old boy with a Group-E RB, where direct visualization of vitreous and subretinal seeds was made under fluorescein stain and compared with the seeds in H and E-stained slide and FESEM. There was full-thickness choroidal involvement in that eyeball with prelaminar optic nerve involvement. The tumor was undifferentiated with extensive necrosis and calcification. The surface pigment change of subretinal seeds and vitreous seeds having honeycomb appearance correlated with the H and E-stained slides' seeds. FESEM-documented seeds could suggest that those surface pigments on subretinal seeds could have local effects in tumor resistance to chemotherapy. RB seed documentation in FESEM has never been reported in the scientific literature previously.

RB calcification in the same case by FESEM showed a lamellar arrangement of osteophytes with fiber orientations that changed from one lamella to the adjacent.[14-16] The remodeling of tumoral calcification observation in RB calcification was also not documented by FESEM previously in the literature, as in our case in the study.[14-16]

Noninfrared Raman spectroscopy in our study showed important findings between normal adjoining tissue and a group of RB seeds. Spectra of normal tissue showed less spectral spikes, whereas RB seeds showed characteristic high spikes. This can be attributed to normal tissue that has more lipids content, whereas malignant RB seeds have higher protein by-products expressed by the tumor. Raman spectroscopy can map useful cellular chemico-physical microenvironment of the tumor.[17-20] Raman-based probe already detected cancer cells in brain with 93% sensitivity and 91% specificity.[18-20] Raman spectroscopy is used in real-time mode in tumor samples where solid cancer seeds were seen.[18-20] Raman spectra can distinguish malignant tumor from the benign tumor with considerable accuracy.[18-20] There can be distinguishing points between benign, malignant, inflammatory, and transforming tumor (reactive lymphoid hyperplasia into full-blown lymphoma) in real time in this spectral study and can be newer innovation in cancer diagnosis.[18-20] In future thought, real-time spectroscopy devices mounted on slit-lamp biomicroscopy or endoscopy can give evidence of cancer in the local sites.

Conclusion

This pathological study on RB seeds showed various high-risk factors associated with the tumor seeds. Characteristic surface change of these subretinal seeds could be associated with RB chemotherapy resistances that require future validation. FESEM and Raman spectroscopy in an index case RB seeds has opened up a new frontier to ocular tumor imaging in the future.

Acknowledgments

The authors wish to express their thanks to Sri Kanchi Sankara Health and Educational Foundation, India; Prof. Gautam Biswas, Ex-Director, IIT Guwahati; Prof. Panna Deka, MD; Dr. Ganesh Chandra Kuri, MS; Mr. Pankaj Kumar Goswami, MSc; and Matrix Imaging.

Financial support and sponsorship

Nil.

Conflicts of interest

There are no conflicts of interest.

References

1. Tamboli A, Podgor MJ, Horm JW. The incidence of retinoblastoma in the United States: 1974 through 1985. Arch Ophthalmol 1990;108:128-32.
2. Vemuganti G, Honavar S, John R. Clinicopathological profile of retinoblastoma patients in Asian Indians. Invest Ophthalmol Vis Sci 2000;41:790.
3. Shields CL, Shields JA, Donoso LA. Clinical genetics of retinoblastoma. Int Ophthalmol Clin 1993;33:67-76.
4. Eagle RC Jr. Eye pathology: An Atlas and Text. 2nd ed. Philadelphia: Wolters Kluwer/Lippincott Williams and Wilkins; 2011.
5. Seregard S, Singh AD. Retinoblastoma: Direct chemotherapeutic drug delivery into the vitreous cavity. Br J Ophthalmol 2012;96:473-4.
6. Biswas J, Das D, Krishnakumar S, Shanmugam MP. Hisopathological analysis of 232 Eyes with retinoblastoma conducted in an Indian Tertiary- Care Ophthalmic center. J Pediatr Ophthalmol Strabisums 2003;40:265-7.
7. Eagle RC Jr. High-risk features and tumour differentiation in retinoblastoma: A retrospective histopathologic study. Arch Pathol Lab Med 2009;133:1203-9.
8. Das D, Bhattacharjee K, Barthakur SS, Tahiliani PS, Deka P, Bhattacharjee H, *et al*. A new rosette in retinoblastoma. Indian J Ophthalmol 2014;62:638-41.
9. Sastre X, Chantada GL, Doz F, Wilson MW, de Davila MT,

Rodríguez-Galindo C, *et al*. Proceedings of the consensus meetings from the International Retinoblastoma staging working Group on the pathology guidelines for the examination of enucleated eyes and evaluation of prognostic risk factors in retinoblastoma. Arch Pathol Lab Med 2009;133:1199-202.

10. Das D, Deka P, Bhattacharjee H, Deshmukh S, Gupta P, Deka A, *et al*. Fluorescein dye as a novel cost-effective approach for staining raw specimens in ophthalmic pathology. Indian J Ophthalmol 2020;68:2175-8.
11. Honavar SG, Singh AD, Shields CL, Meadows AT, Demirci H, Cater J, *et al*. Postenucleation adjuvant therapy in high-risk retinoblastoma. Arch Ophthalmol 2002;120:923-31.
12. Munier FL. Classification and management of seeds in retinoblastoma. Ellsworth Lecture Ghent August 24th 2013. Ophthalmic Genet 2014;35:193-207.
13. Das D, Deka P, Biswas J, Bhattacharjee H. Pathology of retinoblastoma: An update. In: Nema HV, Nema N, editors. Ocular Tumors. Singapore: Springer; 2021. p. 45-59.
14. Craft JL, Robinson NL, Roth NA, Albert DM. Scanning electron microscopy of retinoblastoma. Exp Eye Res 1978;27:519-31.
15. Albert DM, Craft J, Sang DN. Ultrastructure of retinoblastoma: Transmission and scanning electron microscopy. In: Jakobiec FA, editor. Ocular and Adnexal Tumors. Birmingham: Aesculapius Publishing Company; 1978. p. 157-71.
16. Sela J. Bone remodeling in pathologic conditions. A scanning electron microscopic study. Calcif Tissue Res 1977;23:229-34.
17. Raman CV, Krishnan KS. A new type of secondary radiation. Nature 1928;121:501-2.
18. Su L, Chen Y, Zhang GN, Wang LH, Shen AG, Zhou XD, *et al*. *In vivo* and *in situ* monitoring of the nitric oxide stimulus response of single cancer cells by Raman spectroscopy. Laser Phys Lett 2013;10:045608.
19. Buckley K, Kerns JG, Parker AW, Goodship AE, Matousek P. Decomposition of *in vivo* spatially offset Raman spectroscopy data using multivariate analysis techniques. J Raman Spectrosc 2014;45:188-92.
20. Pichardo-Molina JL, Frausto-Reyes C, Barbosa-García O, Huerta-Franco R, González-Trujillo JL, Ramírez-Alvarado CA, *et al*. Raman spectroscopy and multivariate analysis of serum samples from breast cancer patients. Lasers Med Sci 2007;22:229-36.
21. Mendoza PR, Specht CS, Hubbard GB, Wells JR, Lynn MJ, Zhang Q, Kong J, *et al*. Histopathologic grading of anaplasia in retinoblastoma. Am J Ophthalmol 2015;159:764-76.